Modeling Airflow and Lift to Design a Wing for Human-Powered Flight

Alan Bruner, Evan Cochrane, Theodore Guetig, Ben Wilfong

Introduction

In the digital age, using computers for modeling and design work is vital to conserve time and resources. In aerospace applications, modeling software is used to evaluate current digital designs and further their development before implementing a physical prototype. This process is known as digital engineering and is becoming a common practice in industry, including the United States Air Force. To better understand the push towards digital engineering, we will design a human-powered aircraft by computing the lift generated by its wings using the computational software MATLAB. The panel method is used for this task due to its low computational cost relative to a computational fluid dynamics approach. Panel methods provide accurate calculations of lift, but are unable to provide drag estimates.

Model

The power generated by a human is limited relative to that of an internal combustion engine. For this reason, human-powered flight requires careful selection of an airfoil that offers high lift coefficients at low speeds. The DAE11 airfoil was selected because it meets these desired characteristics and was implemented on the Daedalus project, which holds the current record for longest human-powered flight [3]. Additionally, the simple panel method will be used to represent the DAE11 airfoil. This model does not include any complex geometry or changing structural characteristics.

Image Processing

Before running the computational model, the airfoil data points need to be extracted and loaded into MATLAB. Once the image is loaded, a Sobel edge filter is applied, which can determine the general shape of the wing in the image. This edge detection will likely leave gaps, so the output of the Sobel filter is then fed through a dilation function. This will ensure the edge is a single continuous shape.

The next step is to find the perimeter of the edge feature, which is then converted to a list of points. To do this, the image is first passed through a fill

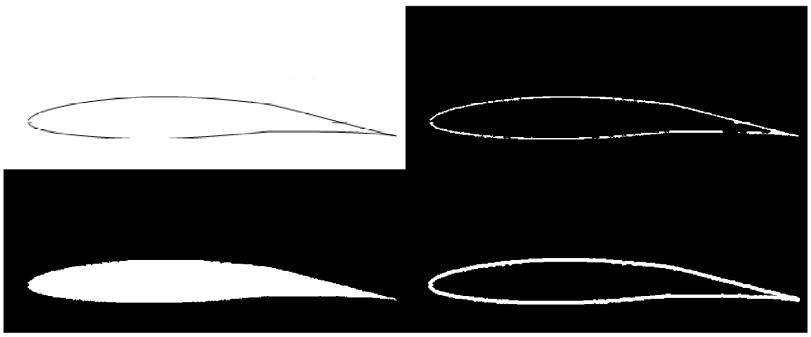

Figure 1: The steps taken to process an image. **Top Left:** The original image **Top Right:** The results from the edge filter **Bottom Left:** The filled edge filter **Bottom Right:** The perimeter of the object

function, which will replace the interior of the edge with true values. This is necessary to do before using MATLAB's **bwperim** function, which will return an image with true values only along the perimeter of any shapes in the image. Without filling the image, this function will return true on both the inner and outer sides of the dilated edge filter. Once the perimeter is found, the function **bwtraceboundary** can be used to return an in-order list of all points along the perimeter, starting at the lower right corner, which is used to create the wake trail. Figure 1 shows the steps taken when processing an image.

Once all image pre-processing is done, the data points themselves can be found. This is done by tracing over the perimeter of the processed image, and using an angle tolerance to determine when a new point should be placed. When a new point is placed, the function moves a number of pixels along the perimeter, and calculates the angle between those two points. The function then continues along the perimeter, calculating the angle between the current location and the previously placed point at each step. If the current calculated angle is outside of a specific tolerance, then a new data point is placed at the current location, and a new comparison angle is calculated. This process continues until the entire perimeter has been traced over. This method is done to ensure that more points are placed along areas of the wing with greater curvature, which will provide the most information when running the mathematical model on discretized profile.

In order to allow the user to select how many points the approximation should have, the function dynamically finds an angle tolerance which results in the desired number of points. This tolerance is found using a modified binary search algorithm. If the angle tolerance is too low, then the program will generate more points than desired. If the tolerance is too high, then the program will generate too few points. If too many points are found, the angle tolerance

Figure 2: The resulting points of the point finding algorithm, shown as red crosses

is increased by a factor of two. If too few points are found, the angle tolerance is decreased by half of the possible ranges of angles. This process repeats until the desired number of points are found. Figure 2 shows the resulting points of a sample wing overlaid onto the original image.

Once the desired number of points are found, the program adds two more points: a repeat of the first point, and a point to represent the wake trail. The location of the wake trail point can be defined by the calling function in terms of the length of the wake trail and the angle created from the horizontal of the trail. This allows the calling function to customize the wake trail, depending on the orientation of the wing.

Mathematical Model

We use the symbol Φ to denote the airflow at a given point in two-dimensional space with coordinates x and z, so the gradient $\nabla\Phi$ represents the velocity of the fluid at a given point. Over a region R, the rate at which the mass of fluid changes with time can be computed using the formula

$$\frac{dm}{dt} = \frac{\partial}{\partial t}\int_R \rho\, dV - \int_{bd(R)} \rho\nabla\Phi\mathbf{n}\, dS, \tag{1}$$

where $bd(R)$ is the boundary region of R, $\mathbf{n}$ is an outward facing normal vector, and ρ is the density of the air [1]. A number of simplifying assumptions are made to allow us to derive a formula for $\nabla\Phi$. First, we assume air is incompressible and homogeneous, i.e., constant density, so ρ is constant everywhere, and

$$\int_R \rho\, dV = 0.$$

We also know that the mass of the region does not change, $\frac{dm}{dt} = 0$, reducing (1) to

$$\int_{bd(R)} \nabla\Phi\mathbf{n}\, dS = 0.$$

By the divergence theorem, then,

$$\int_{bd(R)} \nabla\Phi \mathbf{n}\, dS = \int_R \nabla^2\Phi\, dV = 0. \tag{2}$$

The second integrand in (2) must be 0 if the integral is 0, which gives Laplace's equation for incompressible flow,

$$\frac{\partial^2\Phi}{\partial x^2} + \frac{\partial^2\Phi}{\partial z^2} = 0.$$

The only solutions to Laplace's equation are sources, sinks, and doublets. The streamlines for these solutions look like:

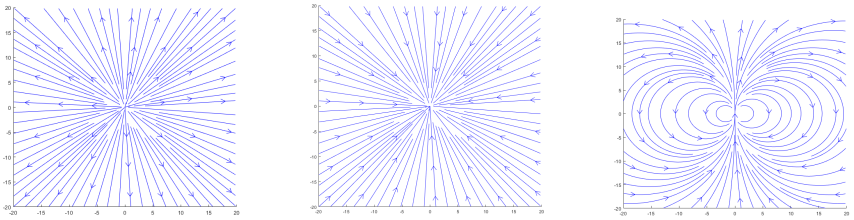

(a) (b) (c)

Figure 3: Source (a), sink (b), and doublet (c) solutions to Laplace's equation.

When modeling a wing, we only consider the doublet solutions Φ_d close to the wing and assume a known constant free stream velocity Φ_f far from the wing. The doublets are oriented so that a flat wing surface would be horizontal in the center of the picture in Figure 3(c). Our streamline calculation is then

$$\Phi \approx \int_C \mu\Phi_d\, dl + \Phi_f,$$

where C is a curve defining the two-dimensional wing cross-section and μ is the doublet strength. We can approximate the streamline by replacing C with N linear panels, including a wake panel at the tail of the wing. This gives

$$\Phi \approx \sum_{j=1}^{N} \int_{L_j} \mu_j\Phi_d\, dl + \Phi_f, \tag{3}$$

where each L_j is a panel.

We use the boundary assumption

$$\mathbf{n}\nabla\Phi = 0, \tag{4}$$

which roughly corresponds to the velocity vectors being tangent to the wing, to solve for each doublet strength, assuming a constant doublet strength for each panel μ_j. Substituting (3) into (4) for each panel i gives

$$\sum_{j=1}^{N} \mu_j (\mathbf{n}_i \int_{L_j} \nabla \Phi_d \, dl) + \mathbf{n}_i \nabla \Phi_f = 0.$$

We then formulate this as a system of linear equations,

$$A\boldsymbol{\mu} = \mathbf{b},$$

where $\boldsymbol{\mu}$ is the vector of doublet strength to solve for,

$$A_{ij} = \mathbf{n}_i \int_{L_j} \nabla \Phi_d \, dl, \text{ and } \mathbf{b}_i = -\mathbf{n}_i \nabla \Phi_f.$$

All that is left to do now is solve for each integral in the matrix A, and then solve the system. An exact solution to each integral can be found by rotating and translating the wing for each L_i so that panel L_i is centered on the x axis with normal vector pointing in the $-z$ direction. We let d_i denote half of the length of panel i. When $i = j$, the integral is simply

$$\int_{L_i} \nabla \Phi_d \, dl = \begin{bmatrix} 0 \\ \frac{-1}{\pi d_i} \end{bmatrix}.$$

Otherwise, we need to make use of a collection point on panel j, say (x, z). Using the midpoint of each panel as the collection points, the integral for each i gives

$$\int_{L_j} \nabla \Phi_d \, dl = \frac{1}{2\pi} \begin{bmatrix} \frac{z}{(x+d_j)^2+z^2} - \frac{z}{(x-d_j)^2+z^2} \\ \frac{x-d}{(x+d_j)^2+z^2} - \frac{x+d_j}{(x+d_j)^2+z^2} \end{bmatrix}$$

Using a point other than the midpoint gives a significantly longer formula, which we omit for brevity. Of course, these vectors need to be rotated and translated back to their original positions before being dotted with the normal vector and used in A.

Once $\boldsymbol{\mu}$ is solved for, we approximate the circulation arround the wing Γ as the negative of the doublet strength of the wake panel, $\Gamma = -\mu_N$. By the Kutta-Joukowski Theorem, we can estimate the lift generated per meter of wing with a given cross-section as

$$F_l = \Gamma v \rho,$$

where v is the magnitude of the free stream vector and ρ is the density of the air. If the weight per meter of the wing is w_{wing}, and the weight of the fuselage is w_f, we finally estimate how long our wing is going to need to be L to counteract the weight of the plane by solving

$$L w_{wing} + w_f = L F_l$$

for L.

Results

Initial results of lift as a function of wing collection point for the second example in Chapter 8.3 of [1] included one or more singularities due to numerical instabilities in the model. To smooth the results, a cubic spline was fit through one-tenth of the points in the regions of relatively slow change while regions near singularities were omitted. Figure 4 shows the results of this smoothing for the second example from the text with a wake angle of ten degrees. Figure 4a shows the spline points as blue dots along the original curve. The omitted regions are those shaded in light blue. The resulting cubic spline is shown along with the original curve in Figure 4b. These results are representative of those

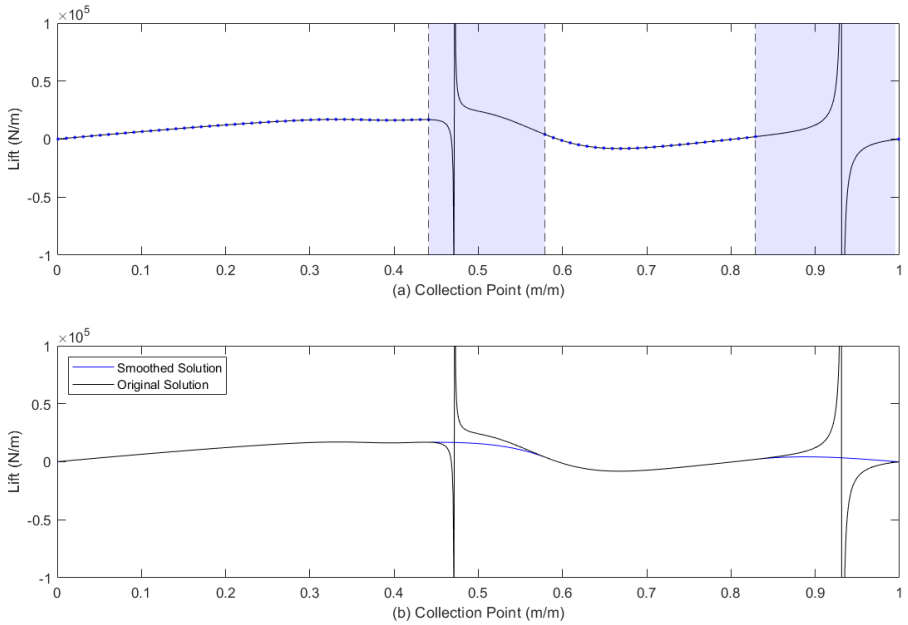

Figure 4: Representative Sample of Spline Points

achieved in all trials.

To study the effects of the wake mode, the wake's length, angle, and collection point were all varied. The results from this search are used to inform an initial guess so that a constrained optimization problem can be used to maximize lift. For each trial, the lift is calculated as a function of the collection point on the main body of the wing with the intent to find a wake model and collection point that maximizes lift.

The first experiment explored the effect of wake angle on lift. To do this, the model was solved for wake angles ranging from ten to seventy degrees below horizontal in ten degree increments while the wake length and wake panel collection point were held constant at 0.957 m and the midpoint of the wake, respectively. The graphical results of this exploration are provided in Figure

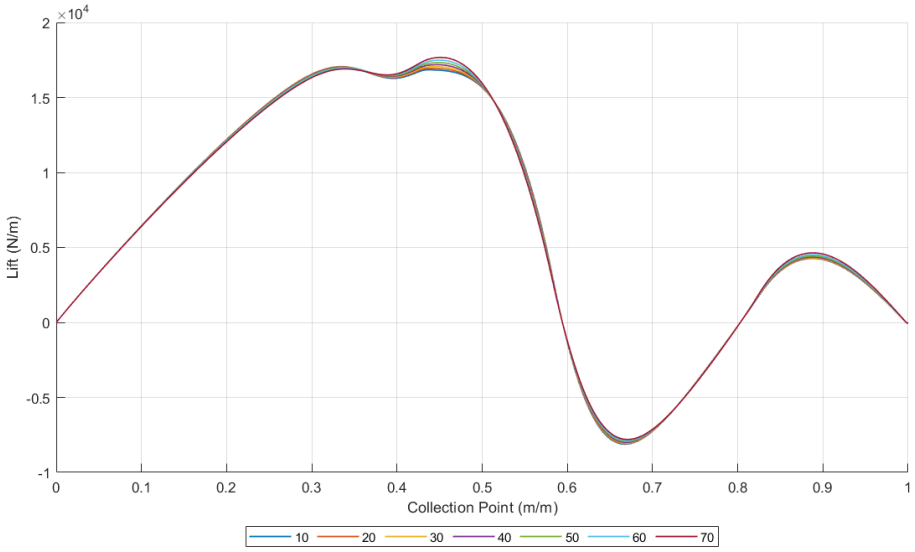

Figure 5: Lift Versus Collection Point for a Range of Wake Angles

5. Table 1 summarizes the maximum lift values for each wake angle and the corresponding wing panel collection point.

Table 1: Wake Angle Summary

Wake Angle	10	20	30	40	50	60	70
Lift (kN/m)	17.05	17.06	16.99	17.01	17.06	17.18	17.33
Collection Point	0.334	0.335	0.444	0.447	0.449	0.450	0.451

Adjusting the wake angle had a relatively small effect on overall lift yielding a range of maximum lifts of only 340 N/m. The trend in maximum lift as a function of wake angle indicates a monotonically increasing lift trend for angles greater than 30 degrees. Examining the wing panel collection points also indicates that at low wake angles, the maximum lift occurs when collection points closer to the front of the wing panels are used. For wake angles of 10 and 20 degrees below horizontal, the maximum lift occurs at the first peak in Figure 5. Beginning with a wake angle of 30 degrees below horizontal, the wing panel collection point corresponding to the maximum lift moves farther back on the panels, corresponding to the second peak in Figure 5.

The second experiment explored the effect of wake length on lift. To do this, the model was solved for wake lengths ranging from 0.2 to 1.1 meters in 15 cm increments while wake angle and wake penel collection point were held constant at 30 degrees and 0.5 respectively. The graphical results of this exploration are provided in Figure 6. Table 2 summarizes the maximum lift values for each wake length and the corresponding collection point on the wing panels.

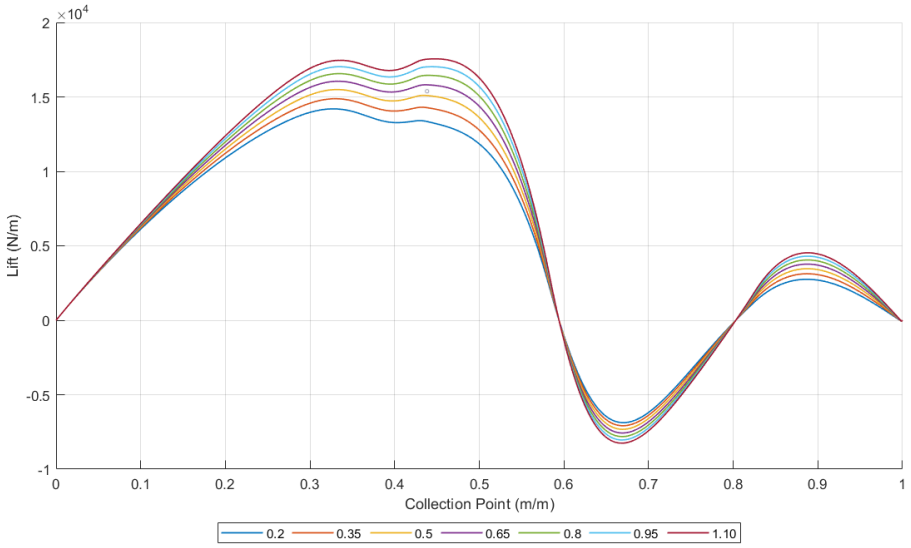

Figure 6: Lift Versus Collection Point for a Range of Wake Lengths

Table 2: Wake Length Summary

Wake Length	0.2	0.35	0.5	0.65	0.8	0.95	1.10
Lift (kN/m)	14.20	14.88	15.49	16.05	16.56	17.03	17.31
Collection Point	0.328	0.330	0.332	0.333	0.334	0.335	0.448

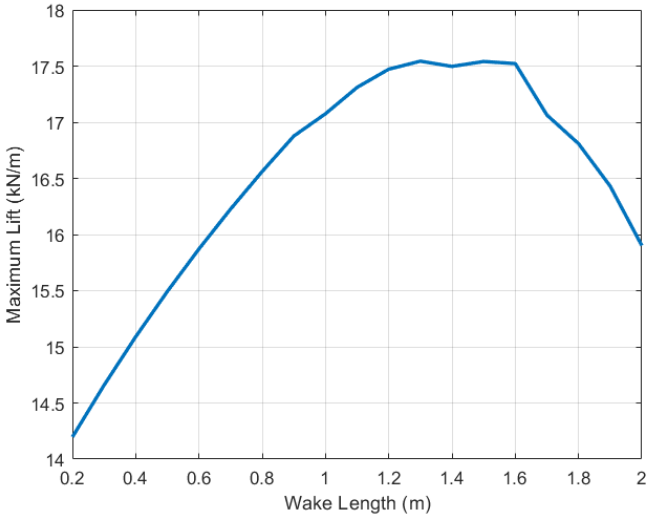

Figure 7: Maximum Lift vs. Wake Length

Table 3: Wake Collection Point Summary

Wake Collection Point	0.5	0.6	0.7	0.8	0.9
Lift (kN/m)	16.99	16.42	15.96	15.61	15.33
Collection Point	0.444	0.332	0.330	0.328	0.327

Adjusting the wake length had a larger effect on lift values than wake angle, yielding a range in maximum lift values of 3.11 kN/m. Extending the maximum wake length to 2 meters yields the trend in maximum lift versus wake length trend shown in Figure 7. By extending the wake length further, a local maximum in lift of 17.54 kN/m is achieved at 1.3 meters. The maximum lift remains relatively constant between 1.3 and 1.6 meters before beginning to decrease.

The third experiment explored the effect of the wake panel collection point on lift. To do this, the model was solved for wake panel collection points ranging from 0.5 to 0.9 in 0.1 increments while wake angle and length were held constant at 30 degrees and 0.957 m respectively. The graphical results of this exploration are provided in Figure 8. Table 3 summarizes the maximum lift values for each wake length and the corresponding collection point on the wing panels.

The wake panel collection point had a relatively large effect yielding a range of maximum lift values of 1.66 kN/m. As the wake panel collection point moves towards the back of the panel, the optimal wing panel collection point moves closer to the front of the panel. Lift as a function of wing panel collection point was very unstable for wake panel collection points less than 0.5. This is why only the range from 0.5 to 0.9 was explored. In this range, maximum lift monotonically decreases with wake panel collection point.

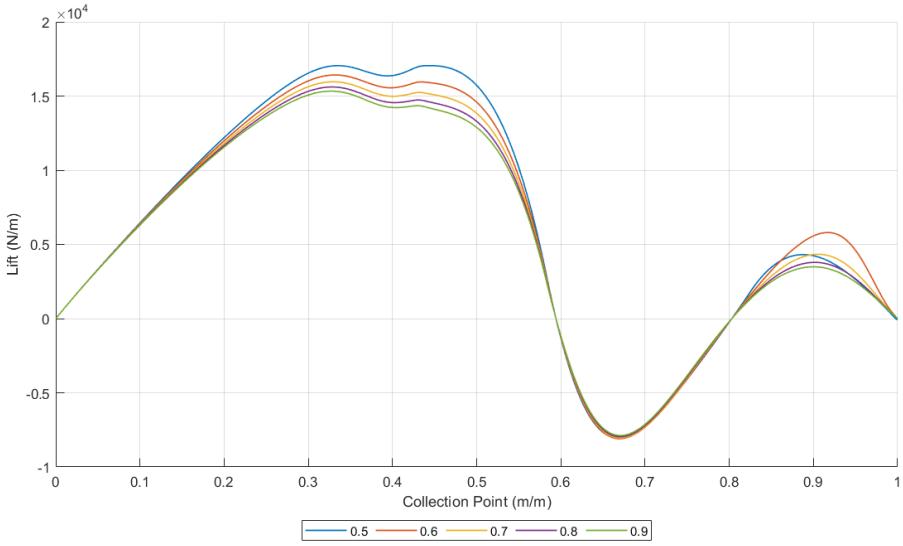

Figure 8: Lift versus Collection Point for a Range of Wake Collection Points

Table 4: Summary of Parameter Results

Parameter	Max (kN/m)	Std. Dev. (N/m)
Angle	17.3	119.5
Length	17.3	1142.3
Collection Point	17.0	660.6

Table 4 summarizes the maximum lift value and standard deviation of the maximum lift values that resulted from modifying each parameter. Wake length was shown to have the greatest effect on maximum lift, followed by wake panel collection point and wake angle. The results of these three experiments suggests a wake model that produces maximum lift without distorting the wing should occur when the wake angle is near 30 degrees below the horizontal, the wake length is near 1.3 m, and the wake panel collection point is near 0.5.

The results of these experiments were then used to define a constrained optimization problem to determine what parameter values yield maximum lift. The following constraints were applied to the parameters:

$$0 \text{ degrees} \leq \text{Wake Angle} \leq 45 \text{ degrees}$$

$$0.2 \text{ m} \leq \text{Wake Length} \leq 2 \text{ m}$$

$$0.5 \leq \text{Wake Collection Point} \leq 0.9$$

The resulting maximum lift of 18.77 kN/m occurred when the wake angle was 35.9 degrees below horizontal, the wake length was 1.997 meters, and the wake

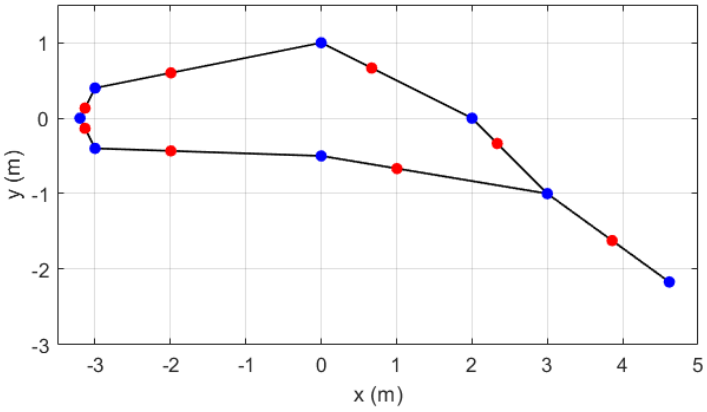

Figure 9: Optimized Panel Model

panel collection point was 0.5313. The wing panel collection point for this lift value was 0.335. The discretized cross-section is shown in Figure 9.

To aid in the design of a human powered aircraft, a 10 panel model is applied to the DAE11 airfoil described previously with a chord length of 2.5 meters, wake angle of 35.9 degrees below horizontal, a wake length of 0.83 meters, a wake panel collection point of 0.5313, an angle of attack of 5 degrees, and a free stream velocity of 6.7 m/s. The results of lift as a function of wing panel collection point are shown in Figure 10 below.

There are two local maximimums in lift. The first is at a wing panel collection point of 0.384 yielding a lift of 37.11 N/m. The second is at a wing panel collection point of 0.794 yielding a lift of 41.97 N/m. At a wing panel collection point of 0.75, commonly used for these problems, the lift is 38.97 N/m. The maximum wing length can then be calculated given the fuselage mass, the passenger mass, and mass per unit length of the wing structure. The required length is given by the following equation:

$$L = \frac{w_f + w_p}{F_l - w_{wing}}$$

where L is the length of the wing, w_f is the fuselage weight, w_p is the passenger weight, F_l is the lift force per unit length produced by the wing, and w_{wing} is the weight per unit length of the wing. For a fuselage weight of 32 lbs (142 N), a passenger weight of 160 lbs (711 N), and a wing mass per unit length of 5.2

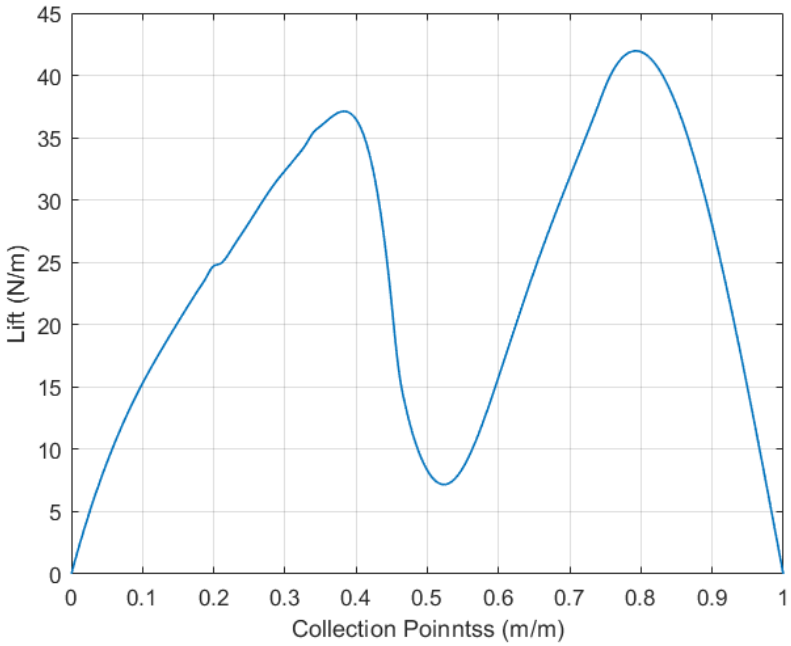

Figure 10: Lift Versus Collection Point

Table 5: Wing Length at Specific Collection Points

Collection Point	F_l (N/m)	L (m)
0.384	37.11	26.73
0.750	38.97	25.26
0.794	41.97	23.20

N/m inspired by the Daedalus project [2], this equation becomes

$$L = \frac{853}{F_l - 5.2}.$$

The required wing length for each collection point is tabulated in Table 5.

The peak in lift that occurs at a wing panel collection point of 0.794 is very sensitive to the region omitted from the cubic spline. The previous experiments suggest that maximum lift will occur when the wing panel collection point is near 0.34, so the wing length of 26.73 meters associated with the wing panel collection point of 0.384 will taken to be the required wing length. When compared to the Daedalus Project [2], this results in an aircraft with a relatively short wingspan. There are however vast differences in wing geometries between this simple model and the complex natural shape used in the Daedalus Project. With lift per unit length values of the same order and in the same general vicinity, we are confident that our model provides insightful information regarding airfoil lift.

Conclusion

Our results suggest that the panel method is an adequate model for calculating lift. It does not, however, provide any information on skin friction drag. We calculated a uniform cross-section wing length of 26.73 meters for a DAE11 airfoil at an angle of attack of 5 degrees and a free-stream velocity of 6.7 m/s. In the Daedalus project, a successful human powered craft was created with a wing span of 34.14 meters [2]. The panel method predictions are of the same order of magnitude as this successful example, suggesting the result is reasonable. A major advantage of the panel method, is its computational speed. Past experience suggests that simple two dimensional computational fluid dynamics models can take seconds to minutes to run while the panel method approach takes only fractions of a second. The advantage becomes even greater in higher dimensions.

Summary

Our modeling framework is described in detail above. In summary, image processing was used to generate a set of panel points from an image which were then used to calculate lift via the panel method. By performing this computational analysis, we are able to achieve an approximation of the airfoil properties without construction of a prototype. With the digital model of the airfoil, it barely takes any time to make minor adjustments and see the results. This achieves the pinnacle of digital engineering as it dramatically saves time and resources to test and evaluate models. We can continue to make alteration to the airfoil and aircraft design until we see the desired results. However, these results do not provide an answer but simply point us in the correct direction. Assuming our computational model is accurate, the prototype should not undergo any drastic changes and should easily behave within our expectations.

To develop a reference for the modeling outputs, we will consider an aeronautical analysis of the Daedalus project's fuselage combined with our simple DAE11 airfoil design [2]. At sea level with constant air properties, the estimated drag coefficients range between 0.01 to 0.02 depending on the mounting angle of the airfoil. These values translate to a drag force range of 22.24 N to 26.69 N at a cruising speed of 6.71 m/s. To power the aircraft, a human will operate a bicycle-like mechanism to generate thrust. Since the average fit human can produce approximately 0.27 HP, the propeller will be able to provide at least 44.48 N of thrust. Therefore, we should expect the human-powered craft to overcome the drag force and achieve a necessary lift force for flight. The estimated wing size varies based on the pilot's weight, the weight of the airfoil, and the mounting angle of the airfoil. The selected fuselage has a fixed weight of 140.79 N while the wings add 5.17 N of weight for every meter of wingspan. To obtain a proper size for the wingspan, we must analyze the linear relationship of weight and lift force. We know that flight can only occur when the lift force exceeds the weight force and by setting them equal to each other the required wingspan can be found. Assuming that the pilot's weight is around 711.71 N and the wings are mounted at an angle of 0 degrees, the wings will need to be 89.63 m which becomes structurally problematic. Using the same weight assumption, we can mount the wings at an angle of 5 degrees and reduce their width down to 30.92 m. This value is much more reasonable to implement on an aircraft and matches up well with the wingspan of the Daedalus project, 34.14 m. These values translate to an average 32.74 N of lift per meter of wingspan.

References

[1] Allen Holder and Joseph Eichholz. *An Introduction To Computer Science*. International Series in Operations Research & Management Science. Cham, Switzerland: Springer, 2019.

[2] John McIntyre and Pat Lloyd. *Man's Greatest Flight*. URL: `https://web.mit.edu/drela/Public/web/hpa/SG_HPAG_daedalus.pdf`. (accessed: 03.11.2022).

[3] Airfoil Tools. *DAE-11 Airfoil (dae11-il)*. URL: `http://airfoiltools.com/airfoil/details?airfoil=dae11-il`. (accessed: 03.12.2022).